JOURNAL OF GEOPHYSICAL RESEARCH, VOL. 104, NO. E9, PAGES 21,911–21,924, SEPTEMBER 25, 1999

# Kilometer-scale slopes on Mars and their correlation with geologic units: Initial results from Mars Orbiter Laser Altimeter (MOLA) data

M. A. Kreslavsky[1] and J. W. Head III

Department of Geological Sciences, Brown University, Providence, Rhode Island

**Abstract.** Martian surface slopes were calculated at baselines from 0.4 to 25 km using profiles obtained by the Mars Orbiter Laser Altimeter (MOLA) instrument during the aerobraking phase of the Mars Global Surveyor mission. Median slope is proposed as a characteristic measurement of the typical surface roughness at each corresponding scale. Median slope is favored over RMS slope because it is not influenced by the small number of higher slopes at the upper end of the slope-frequency distribution tail. Median slope complements interquartile scale roughness characterization in that it is more sensitive to smaller baseline slopes. A map of the median slope of the northern hemisphere is presented. Median slopes and their scale dependences are used to characterize typical kilometer-scale roughness for a set of geologic units mapped in the northern hemisphere. This analysis demonstrates that many individual units and groups of units are characterized by distinctive surface slopes and that these characteristics are sufficiently different that they hold promise for use in the definition and characterization of units. Characterization of the slope properties of geologic units provides information useful in the interpretation of their origin and evolution. For example, the generally smooth topography of the diverse Vastitas Borealis Formation subunits is dominated by about 3 km, 0.3° steep features almost indistinguishable in Viking images. The roughness characteristics of this unit differ from those of other geologic units on Mars and suggest some distinctive process(es) of formation and/or modification of kilometer-scale topography common for all subunits. The similarity of roughness characteristics of the several highland plateau units suggests that kilometer-scale topography was largely inherited from the period of heavy bombardment. The northern polar cap and layered terrains are largely very smooth at small scale. The long, steep-sloped tails of the slope-frequency distributions are compared for the dominant terrain types in the northern hemisphere of Mars and are compared with Earth continents. The Vastitas Borealis Formation found in the northern lowlands differs significantly from both cratered uplands and volcanic plains, and these latter two units can be distinguished from each other on the basis of median slope. Terrestrial continents are smoother than cratered highlands but rougher than the Vastitas Borealis Formation and most volcanic plains. An inventory of all observed slopes much steeper than the angle of repose is presented. Steep slopes occur in the upper parts of tectonic scarps, most likely representing bedrock exposures. The presence of extremely steep slopes in the presumably ductile polar cap provides evidence for geologically recent and/or ongoing formation of these slopes.

## 1. Introduction

In 1997-1998 the Mars Observer Laser Altimeter (MOLA) [*Zuber et al.*, 1992; *Smith et al.*, 1998] on board the Mars Global Surveyor spacecraft [*Albee et al.*, 1998] produced over 2.6 million measurements of surface elevation [*Zuber et al.*, 1998]. This initial survey covers the northern hemisphere of Mars, with a high concentration of measurements at high latitudes. The MOLA aerobraking phase data can be accessed through the Planetary Data Systems Geosciences Node at URL http://wwwpds.wustl.edu/mgs/mola. Part of this data set was used by *Zuber et al.* [1998] to produce a topographic map of the north polar region and to study the polar cap topography.

Individual topographic profiles contain significantly more information than an inevitably generalized topographic map and analysis of individual profiles, together with images of the surface, can provide important information about geologic processes and history. For example, MOLA data have been used to assess impact crater characteristics [*Garvin and Frawley*, 1998], characterize the dichotomy boundary [*Frey et al.*, 1998], analyze volcano morphometry [*Head et al.*, 1998a], and test the hypothesis of former oceans and lakes in the northern lowlands [*Head et al.*, 1998b]. However, the large volume of individual data points cannot all be analyzed individually, and statistical characterization of surface topography, such as kilometer-scale surface roughness, can also provide important information complementary to general topography. The choice of a useful set of such statistical characteristics is not a simple task; typically, slope distributions are described in terms of root-mean-square (RMS) slopes, but this approach may not be optimal for the description of slopes using laser altimeter data. *Aharonson et al.* [1998, 1999] proposed the inter-quartile scale

[1]Also at Kharkov Astronomical Observatory, Kharkov, Ukraine.



Paper number 1999JE001051.
0148-0227/99/1999JE001051$09.00

of topography as a general characteristic of 100-km-scale surface roughness and studied the correlation length of topography. In this paper we focus on the surface slopes along MOLA profiles. We show that median slope is a robust statistical characteristic of surface roughness. We compare this approach to others and show how the median slope and its scale dependence can be used to derive some conclusions about different terrain types and geological units on Mars. We also provide an overview of the steepest slopes in the region of Mars thus far surveyed by MOLA.

## 2. Calculation of Slopes

MOLA measured surface elevation with a high vertical accuracy in a set of points along the orbit of the spacecraft. The distance between subsequent points along each pass is about 400 m and changes systematically along the pass because of the elliptical orbit. The distance is maximal near the pericenter of the orbit and seldom exceeds 30% of its typical value. In a very few cases, surface elevation data points are missing. Sometimes these missing points are due to clouds and thus form small, but continuous segments of passes. Other missing points are due to noise or telemetry gaps and thus are scattered along passes. Each height measurement refers to an approximately circular surface area of diameter of 70 – 300 m [*Smith et al.*, 1998]. The footprint diameter depends on the spacecraft elevation and is minimal near the pericenter of the orbit.

For each MOLA surface data point, we calculated the point-to-point surface slope. We consider it as a slope at the same baseline, 0.4 km long, despite small variations of the actual point-to-point distance. We also calculated a set of slope values for a set of longer baselines [*Kreslavsky and Head*, 1999a, 1999b]. Baseline lengths of 0.8, 1.6, 3.2, 6.4, 12.8, and 25.6 km were used. For each point for each baseline, points about one-half-baseline ahead and about one-half-baseline behind were found. The slope between these points was considered as the slope at the given baseline. We excluded points where there were no neighboring points within 30% of the baseline length.

The accuracy of the calculated slope values depends on the accuracy of elevation differences and the accuracy of spatial distances. The absolute accuracy of the MOLA elevation measurements is defined by long-wavelength orbital uncertainties. They do not influence the accuracy of the slope calculations. The accuracy of the elevation difference between nearby points depends on the roughness and tilt of the surface within the footprint and changes from 0.3 m for a flat surface to ~20 m at the steepest sites [*Smith et al.*, 1998]. This corresponds to errors in slopes of 0.05° or ~10%, which is higher for the short baselines, or a few times better for the long baselines.

The absolute accuracy of the MOLA footprint location is of the order of 1 km [*Smith et al.*, 1998]. In most cases we can expect that the deviation of the inferred footprint location from its true position is similar for nearby points. In this case the positioning inaccuracy does not influence the slope calculation precision. However, in some cases, when instrument attitude changes, the error can be significant. Some MOLA profiles were taken with MOLA axes deflected from the local nadir to cover the pole and some other interesting sites. We found that statistics of slopes along these profiles is very different from that along the regular profiles. Figure 1 shows examples of a regular and an off-nadir profile for the same site in the polar cap. The saw-like variations of elevation in the off-nadir profile are probably due to inaccuracy in the knowledge of the

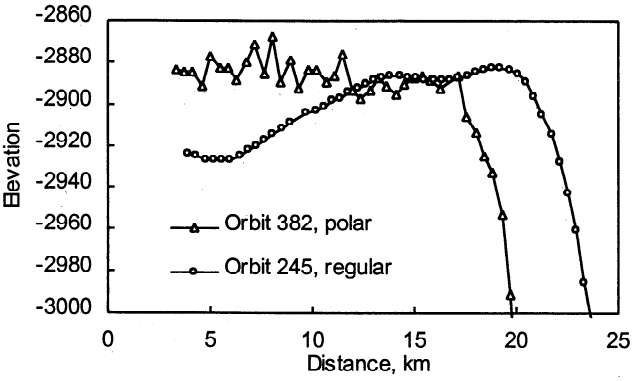


**Figure 1.** MOLA profiles at the site in the polar cap located at 86°N, 240°W. Profile from orbit 245 was taken using the regular geometry with MOLA axis directed to the local nadir. Profile from orbit 382 was taken with off-nadir attitude. Passes are approximately perpendicular to each other and cross somewhere in the center of the plot. The apparent difference in profile pattern is probably due to errors in the axis direction measurements for the off-nadir orbit.

MOLA axis orientation, which leads to errors in the calculation of elevation from the measured slant distance. We excluded all off-nadir measurements from our statistical studies of surface slopes.

The point-to-point distance is not equal to 0.4 km everywhere and changes systematically with latitude. This leads to some systematic deviation of the actual baseline from the ideal one for short baselines. In turn, this leads to a bias in slope statistics. As we learned from the analysis (see below), the dependence of the slope statistical properties on the baseline length varies to a great extent for different geologic units. Hence there is not any straightforward and correct way to introduce a correction for this systematic difference in the baseline. We will see below that the dependence of the median slope on the baseline length can be described with a power law. Typically, the power law exponent is lower than 0.5, although for some unusual geologic units it can be up to 1. Hence the ±30% deviation of the baseline length typically leads to <15% bias in the median slope, though rarely a higher bias is possible. The width of the median slope variation range exceeds an order of magnitude. The described latitudinal bias is small in comparison to this range. We removed all segments that fell outside the ±30% baseline-length range and ignored the bias in our study.

The finite (nonzero) size of the footprint implies some averaging (smoothing) of actual topography. We expect some influence of this effect on statistics of the point-to-the-nearest-point slopes, where the footprint size is comparable to the baseline length. Systematic changes of the footprint size with latitude, especially together with the systematic changes of the point-to-point distance, can lead to another bias in slope statistics. In our analysis of the dependence of the median slope on the baseline length (see below) we do not see any noticeable systematic deflection of the median slope at the shortest baseline from the trend. This means that the effect of the averaging on the median slope is small. In turn, this means that any bias in this effect is negligible.

Examples of cumulative slope-frequency distributions calculated using all available data are presented in Figure 2. The distributions correspond to three selected baselines. The cumula-

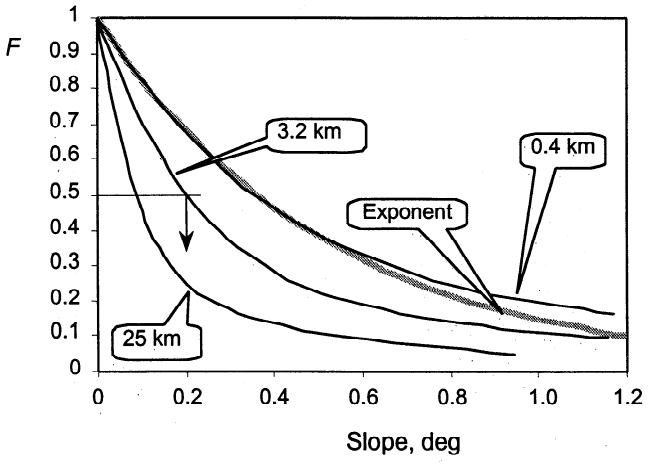


**Figure 2.** Cumulative slope-frequency distribution ($F$) for three baselines. The distributions are calculated using all available good data points. Shown also is an approximation of the 0.4-km-baseline slope distribution with exponential distribution function. The arrow illustrates the definition of the median slope.

tive distribution function $F$ is defined here as the percentage of data points with a slope steeper than that given. Note that these distributions do not represent an "average Mars" because the data points are not spread evenly or randomly over the surface. The distribution functions are rather similar to exponential ones for gentle slopes (Figure 2) and decrease much more slowly for steeper slopes. It is observed that typical surface slopes decrease with increasing baseline length.

## 3. Approach to Characterization of Surface Roughness

Our goal is to characterize the kilometer-scale surface roughness using slope-frequency distribution statistics. In this study we restrict ourselves to "local" statistics. This means that we consider parameters of the slope-frequency distribution in a region or in a profile segment, and do not consider any correlation between neighboring points, which is the subject of future studies. An attempt to apply a nonlocal characteristic of roughness, the correlation length, to the MOLA data was done by *Aharonson et al.* [1998, 1999].

### 3.1. Median Slope

Traditionally, RMS slope is used as a "local" characteristic of surface roughness. For example, *Aharonson et al.* [1998] mapped the RMS slope in a 100-km-wide sliding window along profiles. However, in some situations the RMS slope does not provide a good characterization of typical surface slopes. Such situations are discussed from an elementary mathematical viewpoint, for example, by *van der Vaerden* [1969, section 20]. Our analysis shows that the RMS slope is not a good measure of the surface roughness in the case of MOLA data [*Kreslavsky and Head*, 1999a, 1999b]. The reason for this is that the slope-frequency distribution has a long tail. This means that there are some rare extremely steep slopes. They have a significant effect during the averaging of the squares of slopes. Thus the RMS slope is controlled significantly by the presence of these rare steep slopes, rather than by typical surface slopes.

For example, the typical point-to-point slope for the vast northern plains on Mars is about 0.3°, although there are some impact craters in these plains with slopes as steep as 30°. If a 50-km-long segment of a profile in the northern plains contains only one point with a 30° slope and other points have slopes about 0.3°, the RMS slope for this segment is almost 2°, much steeper than the typical surface slope. Therefore variations of the RMS slope in the northern plains reflect the presence of impact craters, rather than the intrinsic surface roughness of the region or units themselves.

The long tail of the distribution has an additional consequence for the RMS slope. If we increase the number of points for averaging (e.g., enlarge the sample), the probability of finding extremely steep slopes gets higher, and the RMS slope increases. In fact, we did observe this systematic increase of RMS slope with increase in the size of the sample for the same terrain types.

Keeping the disadvantages of RMS slope in mind, several alternative characteristics of surface roughness can be outlined. The mean absolute value of slope is less influenced by the steep-slope tail of the distribution. However, for rough highland terrains on Mars, the slope frequency decreases too slowly with increasing scale of slopes, and mean slope has the same shortcomings as RMS slope.

Another approach is to delete some of the steepest slopes (see Figure 3), for example, the steepest 10% or 20% of the sample, and calculate the RMS slope or the mean slope for the rest of the sample. This eliminates the problem related to the distribution tail. However, the results depend on the onset level, and there is no natural way to define it uniquely.

It is possible to approximate the slope-frequency distribution (except the tail) with some function, for example, the exponent (Figure 2), and use the parameters of the exponent to characterize the roughness. This is a good way until the slope distribution of the sample differs significantly from the model distribution. We found that different units have different distributions. In particular, the global tilt of the surface noticeably distorts the slope-frequency distributions of smooth surfaces.

Rank (order) statistics are a good solution for characterization of typical slopes of the surface. Below we will use the simplest rank statistics, the median absolute value of slope. We will refer this quantity as the median slope. Its definition is illustrated in Figure 2. This characteristic is universal and essentially uninfluenced by the distribution tail.

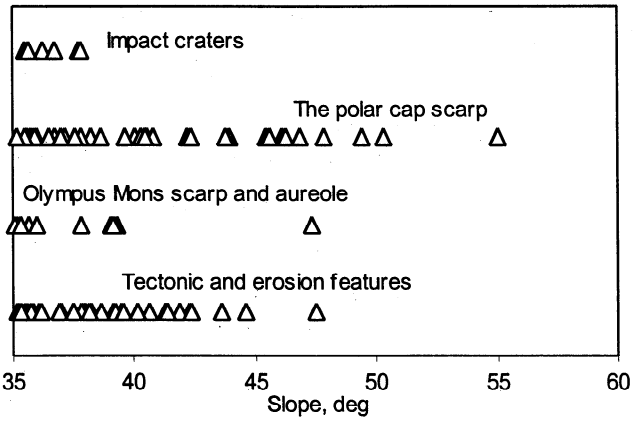


**Figure 3.** The steepest point-to-point slopes from MOLA data grouped according to class of the corresponding features.

Slopes never increase with increasing of the baseline. For virtually all surfaces, slopes decrease with increasing the baseline length. Parameters of this decrease give an essential information about slope statistics.

The median slope at some baseline can be defined by a set of surface features of different scales. On Mars, with its great range of topographic variations, the regional slope can contribute significantly to the median slope values for some terrains. From the value of the median slope alone, it is impossible to distinguish whether this value reflects regional slopes or kilometer-scale surface roughness. Below we will show how the study of the dependence of median slope on baseline length helps to distinguish between these cases.

In treating the statistical characterization of roughness at some scale, one can remove background or regional topography of all larger scales from the slope statistics. In this way, influence of features of different scales on the surface roughness can be more or less effectively separated. However, the choice of the particular definition of what is the "background" or "regional" topography is not obvious. In this analysis we choose not to remove regional slopes, leaving treatment of this problem until global data on longer baseline regional slopes are obtained.

### 3.2. Comparison With the Inter-Quartile Scale

Another rank statistic, the interquartile scale variation of topography (IQS), was proposed as a characteristic of the regional roughness by *Aharonson et al.* [1998]. IQS is the normalized difference between the first and third quartiles of the elevation-frequency distribution. *Aharonson et al.* [1998] calculated IQS in a 100-km-wide window along the MOLA passes.

This statistic deals with the elevation frequency distribution rather than with slope frequency distribution; hence it is a principally different characteristic of roughness. One can create two hypothetical models of stochastically rough surfaces with the same IQS and very different median slopes, or vice versa. However, for natural surfaces it is reasonable to anticipate that rougher surfaces will have both steeper typical slopes and greater topographic variations. For most commonly encountered surfaces, topographic variations at some baseline are due to surface features of a spatial scale of the order of the baseline or somewhat smaller. Hence IQS at some baseline can be anticipated to correlate with slopes at the same baseline or somewhat shorter.

We calculated the IQS in a 50-km-wide sliding window along the passes and compared the results with median slopes calculated in the same window. We found a very close correlation between the IQS and the median slope at the 25-km baseline. This means that the IQS, although a different measurement in principle, characterizes roughness in the same way as the median slope at this baseline. The median slope profiles, in addition to averaging in the 50-km sliding window, have an additional smoothing due to the long (25 km) baseline. As a result, a map of IQS is very similar to a map of 25-km baseline median slope, but has somewhat sharper boundaries. The latitudinal variations of point-to-point distance do not cause any bias in IQS. From the other hand, the median slope allows the treatment of both long-baseline and short-baseline roughness in the same way, up to the baseline equal to the point-to-point distance. The IQS can be calculated only for the baselines containing more than a few points. This factor lead us to chose median slope, rather than IQS, for this study.

### 3.3. Maps of Surface Roughness

We calculated the median slope for our set of baselines in a sliding 50-km-long window along all 205 of the MOLA passes for the Hiatus and Science Phasing Orbit (SPO) Phases 1 and 2. We then put the results in a polar map projection and interpolated to produce a map. We chose an interpolation procedure that preserved maximal possible resolution of the map, in contrast to cosmetic interpolation. The resolution is about 15 km at high latitudes (55°-87°) where the density of MOLA data points is high. At lower latitudes the resolution is much lower because of the wider spacing of the orbits.

Plate 1 and Figure 4 is a composite image of such maps for 0.4-km baseline (blue), 3.2-km baseline (green), and 25-km baseline (red). Brighter shades denote steeper slopes. Such a presentation allows one to gain an overview of both the general roughness of the surface (brighter = rougher; darker = smoother) and the details of the dependence of the median slope on scale. For example, blue shades in Plate 1 indicate the dominance of small-scale roughness, such as the linear dune fields in Olympia Planitia adjacent to the polar cap (180°). The regional slope at the southern part of Olympia Planitia contains some admixed red color, producing a pink shade. Reddish and brown shades indicate relatively smooth regional slopes and the absence of small-scale roughness (e.g., the inner parts of the polar cap; the northern base of Alba Patera, 90-130°). The break in regional slope at the boundary of Alba Patera is clearly seen. The northern lowlands (Vastitas Borealis) are dark green, showing the general smoothness and dominant 3-km scale of the surface roughness of this region and the Vastitatis Borealis Formation contained within.

Features appearing bright in the map are generally rough. Note that the bright peripheral parts of the polar cap (regions characterized by a steep marginal scarp and deep troughs) are reddish, illustrating their smoothness at small scale. Other bright areas within the northern plains are impact craters and elevated patches of residual ice. These rough objects are greenish in the map, showing the absence of regional slopes. The dichotomy boundary is clearly seen in the map. All areas above the boundary have a bright spotty pattern showing a great variability in roughness, including large-scale slopes (orange shades).

## 4. Roughness of Geologic Units and Its Scale Dependence

### 4.1. Geologic Units

We digitized the geologic maps of Mars [*Scott and Tanaka*, 1986; *Greeley and Guest*, 1987; *Tanaka and Scott*, 1987] in order to select MOLA data points corresponding to specific geologic units. The purpose of this exercise was to determine if individual units or groups of units were characterized by distinctive surface slopes and whether such characteristics were sufficiently different that they could be used in the definition and characterization of units, and as an aid in the interpretation of their origin and evolution. Among the units mapped by these authors, we limited our study to geologic units that have sufficient area in the northern hemisphere of Mars to contain more than 10,000 MOLA data points. We excluded segments of MOLA passes located 25 km on both sides of unit boundaries in order to ensure that the whole baselines were located within a specific unit. In addition, this decreased the influence of any

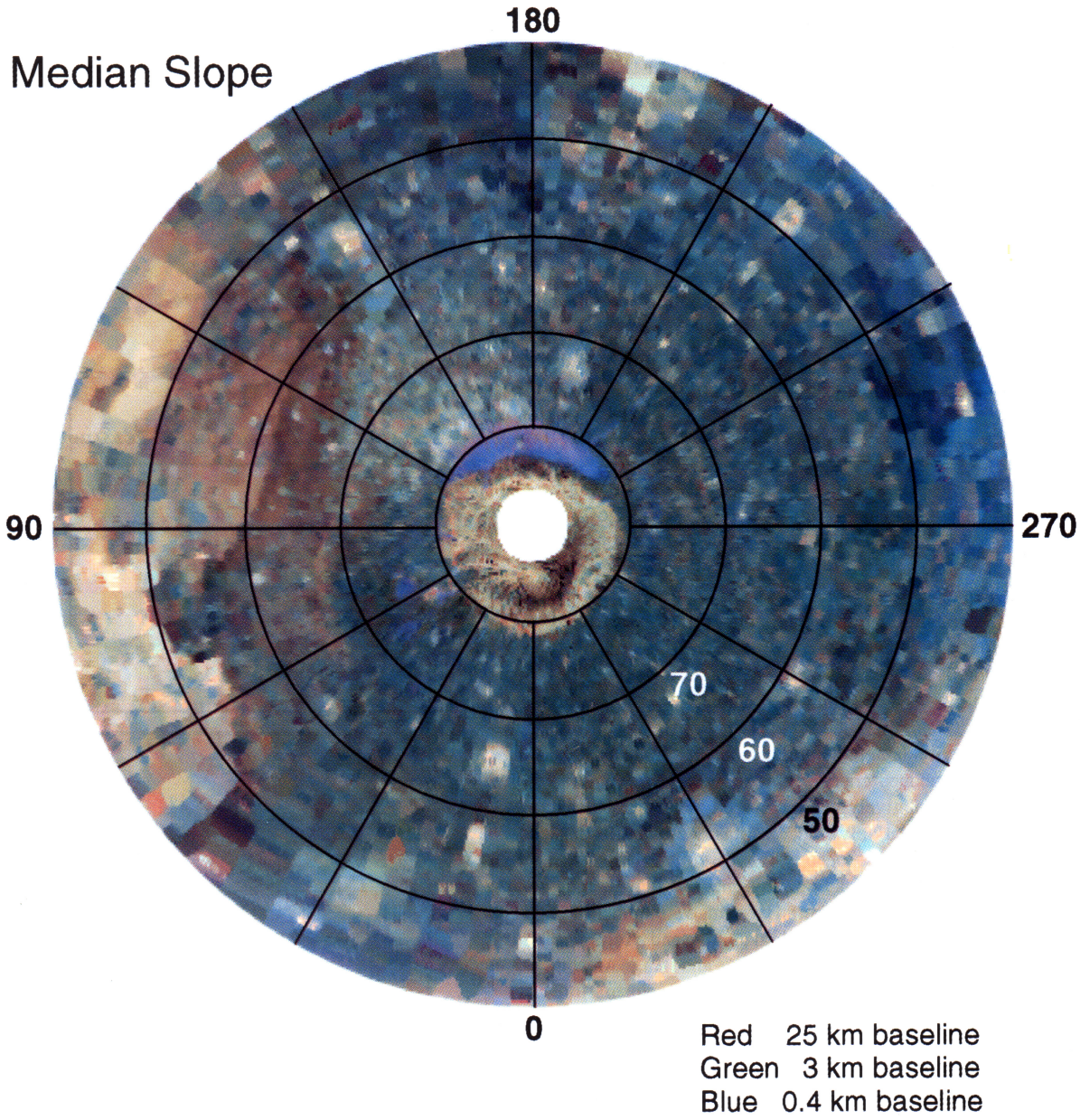


**Plate 1.** Map of median slope in 50 km wide sliding window. Blue channel, 0.4-km baseline; green channel, 3.2-km baseline; red channel, 25-km baseline.

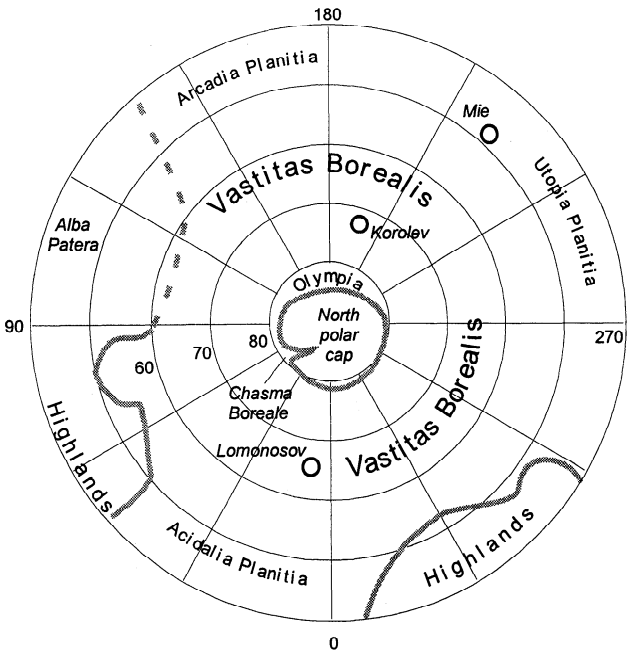


**Figure 4.** Sketch map showing locations of major features and structures.

inaccuracy in locating unit boundaries on digitized geologic maps and their possible geodetic errors. As a result, most of major steep regional topographic slopes, for example, the polar cap scarps and global dichotomy scarp, were excluded from consideration. Thus our statistics reflect the nature of inner or typical roughness of units, rather than topography associated with their boundaries.

The units studied are the following, and more detailed description of the units can be found in the map legends [*Scott and Tanaka*, 1986; *Greeley and Guest*, 1987; *Tanaka and Scott*, 1987]: (1) old heavily cratered highland plateau units: $Npl_1$, cratered unit; $Npl_2$, subdued cratered unit; Npld, dissected unit; Nple, etched unit; (2) relatively old tectonized volcanic plains: Hr, ridged plains; (3) relatively old Vastitas Borealis Formation members, plain units that occupy the vast majority of the northern lowlands on Mars: Hvk, knobby member; Hvm, mottled member; Hvg, grooved member; Hvr, ridged member; (4) different relatively young volcanic plains: $Ael_1$ and $Ael_3$, two members of Elysium Formation; $Aa_1$, $Aa_3$, and $Aa_4$, Arcadia Formation members; Aam, a member of Alba Patera Formation; (5) relatively young plains of uncertain or diverse origin: Apk, knobby plains; Aps, smooth plains; (6) the polar cap material: Api, ice deposits; Apl, layered deposits; and (7) circumpolar plains material: Am, mantling deposits; Adl, linear dune fields.

For each of these units we calculated the median slope for our set of seven baselines. This allowed us to study how typical surface roughness varies with scale.

Comparison of the geologic maps with the roughness map (Plate 1) showed a correlation of changes in roughness and some unit boundaries. Some variations within units were also observed. In this case, the median slope reflects properties of the dominant part of the unit. For example, the patches of remnant ice outside the polar cap (belonging to the Api unit in the map of *Tanaka and Scott* [1987]) are bright green in the roughness map, while the polar cap itself (belonging to the same Api unit) is reddish. In this case the median slope characterizes the typical roughness of the polar cap because the remnants have a much smaller surface area.

Figure 5 shows the relationship of median slope as a function of baseline length for various geologic units, and this provides information on the distinctiveness of units as a whole. Three fundamental observations can be made, as follows.

1) Most units have distinctive characteristics of median slope at these scales and are commonly separable from one another (e.g., the lines do not cross). For example, old heavily cratered highland plateau units are significantly different at all scales from the Vastitas Borealis Formation (compare Figures 5a and 5b).

2) Several units show very tight clustering, suggesting that they share similar slope characteristics. For example, the

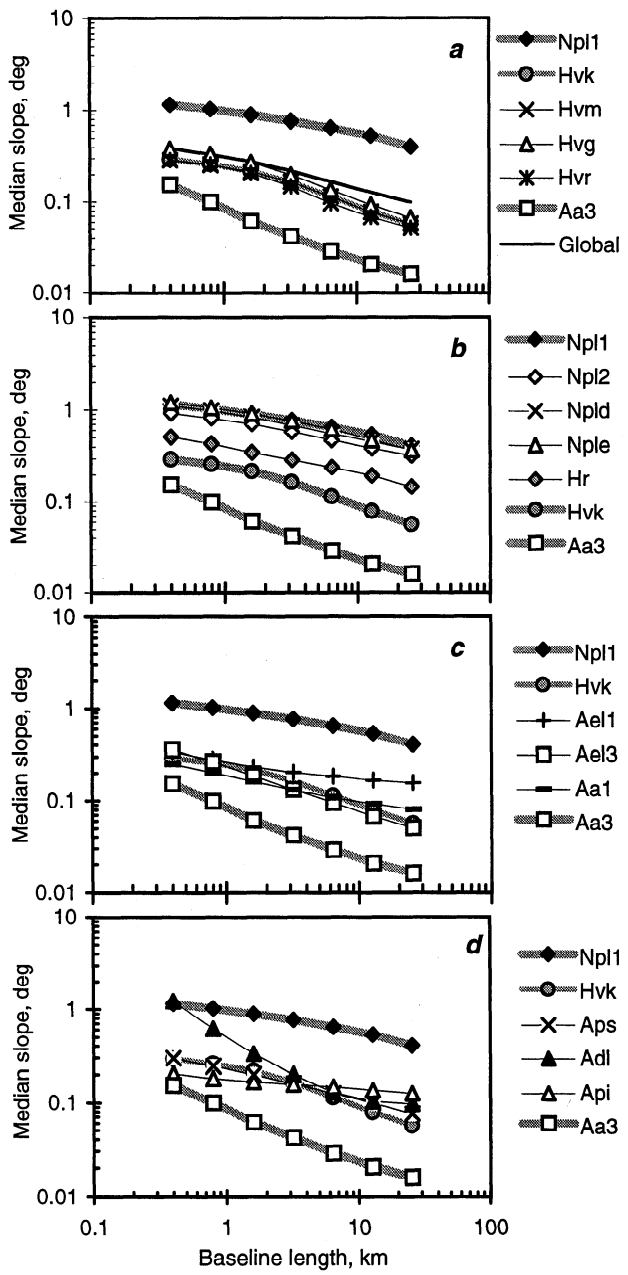


**Figure 5.** Dependence of the median slope on the baseline length for selected geologic units. Logarithmic scale on both axes. The dependence for units $Npl_1$ (typical highland plateau unit), Hvk (typical Vastitas Borealis Formation unit), and $Aa_3$ (extremely flat plains) are shown on all plots (Figures 5a-5d) as a reference.

subunits of the Vastitas Borealis Formation are very similar, despite distinctive morphologic/topographic differences in their definition (grooves, craters, knobs, and ridges).

3) A few units show major variations as a function of baseline length (for example, linear dunes, Figure 5d; see discussion below).

The members of the Hesperian-aged Vastitas Borealis Formation, plains units that occupy the vast majority of the northern lowlands on Mars, are smoother than the global average at all wavelengths. Hvg, the grooved member, is the roughest of the subunits and is rougher at shorter wavelengths, consistent with the presence of pervasive troughs and polygons of a few kilometers across. The old Nectarian-aged heavily cratered highland plateau units (Figure 5b) are tightly clustered and all rougher than the global average at all scales. Among these units, $Npl_2$, the subdued cratered unit, tends to be smoother than the others, consistent with its interpretation as a cratered unit subdued by eolian processes and deposits. The relatively old Hesperian-aged tectonized volcanic plains, Hr (ridged plains; Figure 5b), are much smoother at all scales than the heavily cratered highlands but still uniformly rougher than the global average and all members of the Vastitas Borealis Formation (compare Figures 5a and 5b).

A large number of young (Amazonian-aged) plains units interpreted to be of volcanic origin are seen in this region in Tharsis, Elysium, and portions of the northern lowlands, particularly Arcadia. These units are predominantly smoother than the global average (compare Figures 5c and 5a). Two of these units (Arcadia Formation member $Aa_1$; Elysium Formation member $Ael_3$) fall in the range of the subunits of the Vastitas Borealis Formation. Unit $Aa_1$ is slightly rougher at longer baselines, and this may be due to the fact that it is somewhat older and characterized by the presence of mare-type wrinkle ridges. One member of the Elysium Formation, $Ael_1$, falls in this same group at short baselines but is distinctly rougher at longer baselines, exceeding the global average at baselines in excess of 3 km. The reason for this is related to the fact that this unit appears to be of volcanic origin and derived from the main shields and related vents of the Elysium rise; thus the regional slopes of the rise are observed at longer baselines.

A remarkably smooth unit is observed among this group. The Amazonian-aged member $Aa_3$ of the Arcadia Formation is the smoothest unit observed in the northern hemisphere at all baselines (Figure 5). $Aa_3$ consists of smooth plains that occur west of the Olympus Mons aureoles; these plains embay the aureoles and the nearby fractured terra of Acheron Fossae [*Scott and Tanaka*, 1986] and are the middle member of the Arcadia Formation. This unit shows flow fronts in places and, together with other members of the Arcadia, is interpreted to be of volcanic origin. This unit is younger in age than the Hesperian Vastitas Borealis Formation, which probably underlies it. If so, then the emplacement of these lava flows has smoothed the surface topography of the Vastitas Borealis Formation at all baselines, particularly at the 1-3 km scale so typical of the Vastitas Borealis Formation. These lavas must have an unusual character compared to other volcanic units (Figure 5c), one which is related to smoothness at all scales. In part, this may be due to their emplacement on the already smooth Vastitas Borealis Formation (particularly at longer baselines), but their surfaces must also be very smooth at shorter baselines (hundreds of meters) more indicative of flow surface morphology. Analysis of high-resolution images of nearby Elysium Planitia shows evidence for resurfacing by a very young, thin, apparently very fluid flow unit that appears regionally very smooth, although rough at the few meter scale length [*McEwen et al.*, 1999]. Similar surface characteristics may occur in member $Aa_3$ of the Arcadia Formation.

Amazonian-aged polar units also show distinctive characteristics (Figure 5d). The polar cap material, Api, interpreted as ice deposits, is smoother than the global average except at the longest baseline. In addition, the median slope does not vary significantly as a function of baseline, in contrast to almost all other units. This is almost certainly related to the properties of the ice substrate. Among the circumpolar plains materials occur a variety of mantling deposits, including dune fields [*Tanaka and Scott*, 1987; *Dial*, 1984; *Thomas et al.*, 1992; *Fishbaugh and Head*, 1999]. The linear dune field unit, Adl, is plotted in Figure 5d and is characterized by a very high median slope at short baselines (comparable to the heavily cratered terrain) due to the presence of dunes whose wavelength is in this baseline range, and much smoother surfaces at longer baselines, smoother than the global average but generally rougher than the slopes of the Vastitas Borealis Formation and most volcanic plains.

In summary, this analysis demonstrates that many individual units and groups of units are characterized by distinctive surface slopes (Figure 5), and these characteristics are sufficiently different that they hold promise in the definition and characterization of units. This analysis also shows that further characterization of the slope properties of these and other global units will provide information useful in the interpretation of their origin and evolution. In the future, following circularization of the Mars Global Surveyor orbit, data will be obtained for a wider range of units in the southern hemisphere, including the south polar cap and circumpolar deposits, units within the large impact basins Hellas and Argyre, a range of upland plains of possible volcanic origin, and crater fill units of possible fluvial origin [e.g., *Scott and Tanaka*, 1986; *Greeley and Guest*, 1987; *Tanaka and Scott*, 1987].

## 4.2. Dependence of Median Slope on Baseline Length

Slope values depend on the baseline length. Generally, the shorter the baseline, the steeper the slopes. Figure 5 shows examples of the dependence of median slope (as a characteristic of typical roughness) on the baseline length for a number of geological units. Figure 6 shows some typical examples of profiles. Note that the examples of the profiles are not statistically representative, although they are typical. For example, the steep scarps seen in troughs in the polar cup are absent in the Api profile shown.

It is seen that dependence of median slope on the baseline length displays a wide variety of characteristics over the range of different geologic units. The interpretation of these variations is aided by considering a hypothetical example. Let us imagine a surface formed with some features with a typical spatial dimension $L$ and a typical height $H$. If the baseline length $l$ is much shorter than $L$ ($l<<L$), a typical slope is $H/L$ and does not depend on $l$. This means that there is a dependence of the horizontal segment of median slope versus baseline length. If $l>>L$, the typical slope is $H/l$ and thus is inversely proportional to the baseline length. This translates into an inclined segment of the dependence in the log-log plot with the power law exponent of -1. Of course, real surfaces are formed of vari-

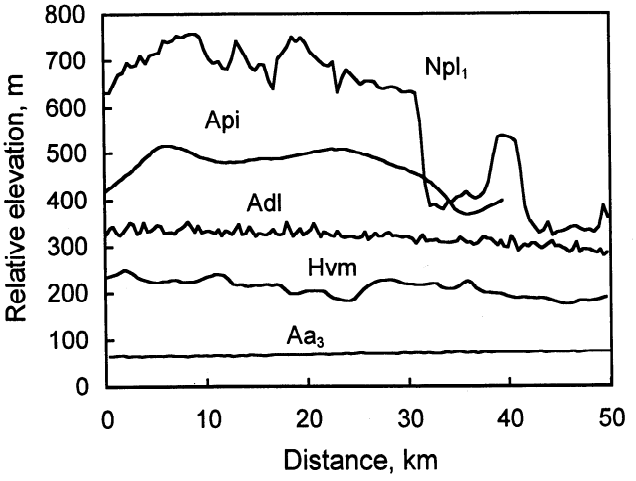


**Figure 6.** Typical segments of MOLA profiles for some units: $Npl_1$, typical profile for heavily cratered highland, orbit 30, 38.5°N, 1.5°W; Hvm, typical profile of Vastitas Borealis Formation, orbit 27, 54.5°N, 245.5°W; $Aa_3$, typical profile of extremely smooth Arcadia Formation volcanic plain, orbit 31, 28.5°N, 160.5°W; Adl, profile across linear dune field, orbit 31, 80.5°N, 138.0°W; Api, typical profile for the polar ice deposits, orbit 32, 81.0°N, 296°W. Profiles are arbitrarily shifted vertically.

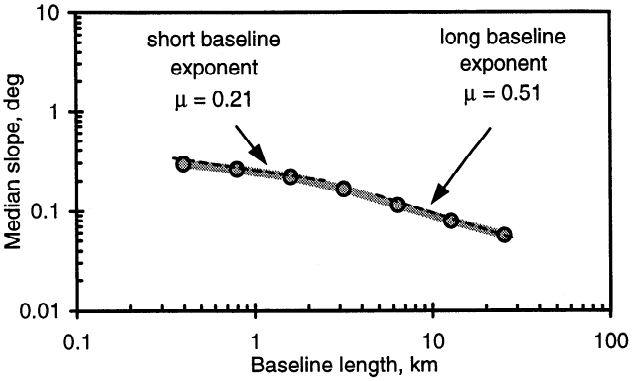


**Figure 7.** Example of the dependence of median slope on baseline (as in Figure 5) showing definitions of short-baseline and long-baseline exponents (unit Hvk).

ous features of different scales. This results in the dependence having different inclinations, between 0 and -1.

For example, for Vastitas Borealis Formation units (Figure 5a), the dependence of the median slope on the baseline length is steeper for longer baselines. This means that at the scale range considered, the topography is dominated by some features with a typical spatial dimension of the order of 3 km (see, for example, profile Hvm in Figure 6). Note that typical values of the correlation lengths obtained by *Aharonson et al.* [1999] for the northern plains are 4-6 km.

Another characteristic example is the Adl unit (linear dune fields in Olympia Planitia). The typical horizontal scale of the dunes is of the order of 1 km or less (Figure 6, profile Adl). The dunes display a very high roughness at the shortest baseline (Figure 5d). The roughness decreases sharply with increasing baseline length (the power law exponent is almost −1). At 6 km baseline, when the median slope becomes as gentle as the regional tilt of Olympia Planitia, the scale dependence almost ceases (Figure 5d). *Aharonson et al.* [1999] obtained a correlation length of less than 1 km for Olympia Planitia.

In order to summarize the variety of dependences of median slope on baseline length, some parameters characterizing the overall dependence would be useful. We approximated the dependence of median slope on baseline length with a power law:

$$\theta_m = \text{const}\ l^{-\mu},$$

where $\theta_m$ is the median slope and $\mu$ is the exponent. We found the best filling power laws separately for short baselines (0.4, 0.8, 1.6 km) and for long baselines (6.4, 12.8, 25.6 km), as illustrated by Figure 7. In Figure 8 we plotted the short-baseline exponent against short-baseline (0.8 km) roughness for the set of units. In Figure 9 the long-baseline exponent is plotted against the short-baseline exponent. The dashed line in Figure 9 marks equal short-baseline and long-baseline exponents in the diagram. Points close to this line correspond to a fractal-like surface roughness. This means that the surface topography is formed by a hierarchy of features of different scales and that no scale is dominant. Areas well above the dashed line in the diagram (low short-baseline and high long-baseline exponents) correspond to surfaces with a dominance of some features of 1-10 km spatial scale. The lower right part of the diagram (high short-baseline and low long-baseline exponents) corresponds to surfaces with a deficit of 1-10 km features, that is with a dominance of small-scale (<1 km) features and regional (>10 km) topography. If there are no small-scale features at all, both exponents are low (lower left corner of the diagram).

### 4.3. Implications for Surface Processes

**4.3.1. Highland plateau.** Figures 8 and 9 show that the roughness of all four highland units ($Npl_1$, $Npl_2$, Npld, Nple) is relatively high and similar at all spatial scales considered (see also Figure 5b). The topography of the highlands is probably largely inherited from heavy bombardment, and morphologically observed traces of erosion, sedimentation and tectonism have not influenced it at these scales. Note that unit $Npl_2$ (subdued cratered unit) is slightly smoother at all scale lengths than the other units, consistent with its somewhat subdued appearance in Viking images.

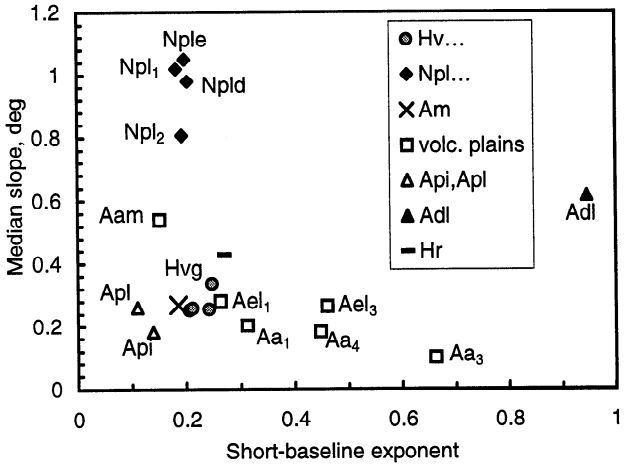


**Figure 8.** Diagram showing the median slope on 0.8 km baseline plotted against the short-baseline exponent for a number of geological units on Mars.

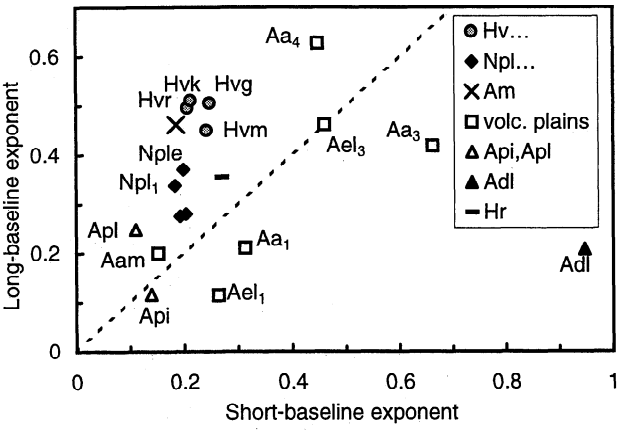


**Figure 9.** Diagram showing short-baseline and long-baseline exponents for a number of geological units on Mars. Dash line marks equal short-baseline and long-baseline exponents (fractal-like surfaces).

**4.3.2. Vastitas Borealis Formation.** All four Vastitas Borealis Formation subunits (Hvk; Hvm; Hvg; Hvr) in the diagrams (Figures 8, 9, see also Figure 5a) are very close to each other despite apparent differences in surface morphology. Observed surface features (knobs, grooves, ridges, rampart craters) contribute little to the slope-frequency distribution and hence do not influence the median slope much. The slope distribution is dominated by ~3 km long ~0.3° steep irregular background features (see examples in Figure 6, curve Hvm). This gentle background topography is almost indistinguishable in the images. The striking similarity of roughness among the varied Vastitas Borealis Formation subunits suggests a possible similarity of surface formation and/or modification processes. One candidate for the formation of these unusual characteristics is that this unit was influenced by the presence of a standing body of water. *Parker et al.* [1989, 1993] hypothesized that the northern lowlands were occupied by a large standing body of water earlier in the history of Mars. Several tests using MOLA data are consistent with this hypothesis [*Head et al.*, 1998a]. Sedimentation from the hypothesized body of water could have smoothed much of the regional topography and perhaps introduced a characteristic scale length not seen on other units of different origin. Other processes that might have contributed to these unusual characteristics include fluvial deposition from the major outflow channels, pyroclastic mantling material from Alba Patera, circumpolar deposit erosion and redeposition, and eolian processes operating on any or all of these deposits.

The circumpolar mantling deposits (Am) are much younger than the Vastitas Borealis Formation and they appear to be thick enough to cover most preexisting craters [*Dial*, 1984; *Fishbaugh and Head*, 1999]. Roughness and its scale dependence for this unit are exactly the same as those of the Vastitas Borealis Formation subunits; Am is in the cluster formed by Hvk, Hvm, Hvg and Hvr units in Figures 8 and 9. These terrains may have been formed by similar repeating or ongoing processes that produced the smoothness of the Vastitas Borealis Formation. For example, Am is interpreted to be formed by sediments derived from sublimation of the permanent ice cap and by sediments from fluvial deposits, both redistributed by eolian processes and covering older cratered plains.

**4.3.3. Volcanic plains.** The volcanic plains display a variety of roughness values. Some of them are noticeably rougher than the Vastitas Borealis Formation, although there are very smooth terrains, for example, the Arcadia Formation unit $Aa_3$, which is much smoother than Vastitas Borealis Formation. However no volcanic plains show the characteristic feature scale of 3 km that is typical of the Vastitas Borealis Formation. This supports the idea that the Vastitas Borealis Formation surface was formed by distinctive surface processes.

## 5. Comparison With Other Data Sets

### 5.1. Comparison With Earth

We used the GTOPO30 digital elevation model of Earth continents (U.S. Geological Survey (USGS), public domain, URL http://edcwww.cr.usgs.gov/landdaac/gtopo30/gtopo30.html, released 20 May 1998) to compare the statistics of slopes with MOLA data. This data set represents ground elevations. GTOPO30 had been produced by compiling of a number of different data sets having different accuracy and resolution. For the purposes of comparison with MOLA data, only two sources used for GTOPO30 production had sufficient resolution and accuracy: Digital Terrain Elevation Data by the National Imagery and Mapping Agency [*Defense Mapping Agency*, 1986] and the USGS digital elevation model [*U.S. Geological Survey*, 1993]. These two sources cover about 70% of the land area. Only GTOPO30 data compiled from these sources were used. The GTOPO30 grid element is about 0.93 km long in the meridian direction; the resolution of the source data sets are much better, and no additional smoothing had been applied when generating GTOPO30 data; hence the GTOPO30 pixel for these source data can be treated as a point measurement of elevation, when the distance between points is greater than pixel size. Thus the shortest possible baseline for these data is 2 pixels, which is 1.9 km in the meridian direction. To calculate slope-frequency distribution in a manner comparable to MOLA data processing, we plotted evenly spaced meridian-directed virtual passes and considered each GTOPO30 pixel as a footprint.

Quantization of the elevation values in GTOPO30 is too rough. This makes it impossible to compare the slope-frequency distribution for gentle slopes. Comparison of the me-

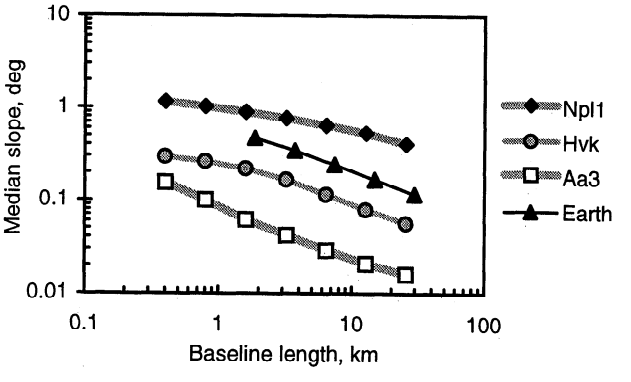


**Figure 10.** Dependence of median slope on baseline length for Earth (GTOPO30 data; see text for details) and Mars (all MOLA data). Logarithmic scale on both axes. Shown also is the extrapolation of the Earth dependence to short baselines used for comparison with the characteristics of geologic units on Mars (Figure 8 and Figure 9).

dian slope and steep-slope distribution tails is possible, however. The dependence of median slope on baseline length for the GTOPO30 and MOLA data are shown in Figure 10. The dependence for Earth is almost linear in the log-log scale (fractal-like behavior) and steeper than for most of the surface units on Mars (Figure 10): the power law exponent absolute value is very close to 0.5. This could also be partly due to gravity differences: for example, gravity-driven ductile relaxation of topography might start for some features of ~10 km spatial scale on Earth but not on Mars. Comparison of these data and examination of Figure 10 show that average Earth continents are smoother than martian highlands and rougher than Vastitas Borealis and the majority of volcanic units on Mars. Parts of the northern lowlands are smoother than Earth's abyssal plains [*Aharonson et al.*, 1998].

### 5.2. Comparison With Other Planets

No presently available topography data for any planet other than Earth are suitable for comparison with slope statistics from MOLA instrument data. For adequate comparison, the topography data should be of a spatial resolution of 1 km or better and an accuracy of a few meters or better. The resolution of direct radar altimeter tracking of Venus [*Ford and Pettengill*, 1992], and Mercury [*Clark et al.*, 1988, *Harmon and Campbell*, 1988] and laser altimeter tracking of the Moon [*Smith et al.*, 1997] is insufficient for direct comparison. All photogrammetric elevation models are based on elevation estimations for a network of irregularly spaced control points. For robust estimation of slope statistics, the typical spacing of the network should be much shorter than the slope baseline. No regional coverage with such high-resolution elevation models is currently available.

### 5.3. Comparison With Radar-Derived Slopes

Indirect estimations of surface roughness using radar technique were widely used for characterization of prospective landing sites on Mars [e.g., *Masursky and Crabill*, 1976; *Simpson et al.*, 1992]. Radar observations provide estimates of the surface roughness at the baselines of the order of several to dozens of the wavelength, that is, 10 cm to 10 m. These baselines are much shorter than MOLA point-to-point distances, and this is why direct comparison of radar measurement and MOLA-derived median slopes is not possible. However, it is extremely interesting to compare extrapolation of MOLA-derived scale dependence of roughness to typical radar baselines.

Interpretation of radar probing results is not straightforward. Although many types of radar experiments gave results in the form of estimates or maps of typical or RMS slope of the surface, the values obtained with different radar techniques are seldom compatible quantitatively. An instructive example was given by *Tyler et al.* [1992]. They processed Doppler-delay arrays obtained with the radar altimeter onboard the Magellan Venus orbiter based on different a priori assumptions about the shape of the backscattering function. Inferred RMS slopes of the surface differed more than twice for different functions taken, although all the methods gave reasonable (and consistent) results about regional roughness variations. Thus one should be aware of probable biases when comparing radar data with direct slope measurements.

An excellent overview of radar data on the martian surface was done by *Simpson et al.* [1992]. Reliable interpretation of radar data in terms of surface slope is possible only if the reflection of microwaves from the surface is well described by the quasi-specular model. Not all terrains on Mars display such radar properties. The "Stealth" region in Amazonis Planitia, for example, is extremely flat and smooth in MOLA profiles [*Aharonson et al.*, 1998] but displays extremely high roughness if the radar data are interpreted through a quasi-specular model. The most likely reason for the unusual radar behavior of this region is subsurface scattering, rather than extremely high meter-scale roughness [*Simpson et al.*, 1992].

As noted by *Simpson et al.* [1992], the scattering properties of the cratered terrains (highland plateau units) are well described by the quasi-specular model with a typical RMS slope about 3°. This value represents typical surface tilts at baselines of about 1-10 m for 12-cm wavelengths. Our study has shown that the highland plateau units display median slope of about 1.1° at the 0.4 km baseline (Figure 5) and a typical short-baseline exponent of about 0.2 (Figure 8). Extrapolation with the power law to 1-10 m baseline gives 3.6°-2.3° slopes, in good agreement with the radar data.

### 5.4. Comparison With MOLA Pulse-Width-Derived Roughness

MOLA pulse width data [*Zuber et al.*, 1992; *Smith et al.*, 1998, *Garvin et al.*, 1999] provide an independent estimation of the differences in the surface elevation within a MOLA footprint. MOLA receiver saturation causes problems with using pulse width data: e.g., "All pulse width acquired when MOLA is in saturation must be discarded" [*Garvin et al.*, 1999]. In addition, for the off-nadir measurements the slant distance depth of the footprint dominates in the reflected pulse width, and the roughness information cannot be extracted. Only 42% of MOLA points in the whole Hiatus+SPO1+SPO2 data set have "good" estimates of the pulse width.

*Garvin et al.* [1999] subtracted the contribution due to along-track slope from the pulse width and obtained vertical roughness. The spatial scale of this roughness estimator is defined by the footprint diameter (180-300 m). Most estimates of the vertical roughness were reported by *Garvin et al.* [1999] to be in the range of 0.5–2.0 m; values up to 6 m were typical, although infrequent. The northern lowlands display a rather uniform vertical roughness of about 0.9 m; small variations over these plains are probably due to measurement noise and may not reflect real changes in surface characteristics.

The vertical roughness (as is also the case with the IQS) deals with distribution of elevations rather than with the distribution of slopes, and hence is a principally different characteristic of the surface roughness. Analogy with the IQS suggests that the vertical roughness might correlate with the slopes at about the half-footprint baseline. The mean value of the vertical roughness for the equatorial uplands reported by *Garvin et al.* [1999] is 2.8 m; this height difference corresponds to 1.6° slope at a 100-m baseline. This slope is close to the 1.5° slope suggested by the extrapolation of the highland plateau median slopes to 100-m baseline (see above). Thus the order of magnitude of typical vertical roughness for the highlands is consistent with kilometer-scale slopes and radar estimates. The situation is different in the northern lowlands. The mean value of the vertical roughness of 0.9 m [*Garvin et al.*, 1999] corresponds to a 0.5° slope at the 100 m baseline, much higher than the 0.08° slope derived by the extrapolation of median slopes for the Vastitas Borealis Formation.

Although high values of vertical roughness are usually attributed to regions of steep topography, the correlation be-

tween kilometer-scale median slopes and the vertical roughness is not close. An example of terrains showing the same median slopes and very different pulse widths was described by *Cooper and Mustard* [1999]. In summary, the pulse width data, if valid, provide information about the surface essentially compatible and complementary to the point-to-point slope data.

## 6. Steep Slopes

### 6.1. Statistics of Steep Slopes

As we described above, the slope-frequency distributions have very long tails. In comparison to the median slope, very steep slopes are typical though not frequent. Examples of the steep-slope tails of the distribution are shown in Figure 11 for a set of geologic units. Both axes in the plots are in logarithmic scales. This type of presentation is useful for comparison of long distribution tails. The steep-slope tails of the distributions contain a small proportion of the data points. With the amount of data available, we have to combine geologic units to obtain good statistics of steep slopes.

The Vastitas Borealis curve in Figure 11 corresponds to most of the northern lowlands (units Hvk, Hvm, Hvg, Hvr, and Am). Vastitas Borealis is deficient in steep slopes, and the frequency distribution slope change is seen at about 0.5°-2° (Figure 11). The rare steeper slopes are probably related to fresh impact craters and are not typical for this terrain. The typical few-kilometer-scale topographic features forming the surface of Vastitas Borealis (Figures 5b, 8, 9) never have steep slopes.

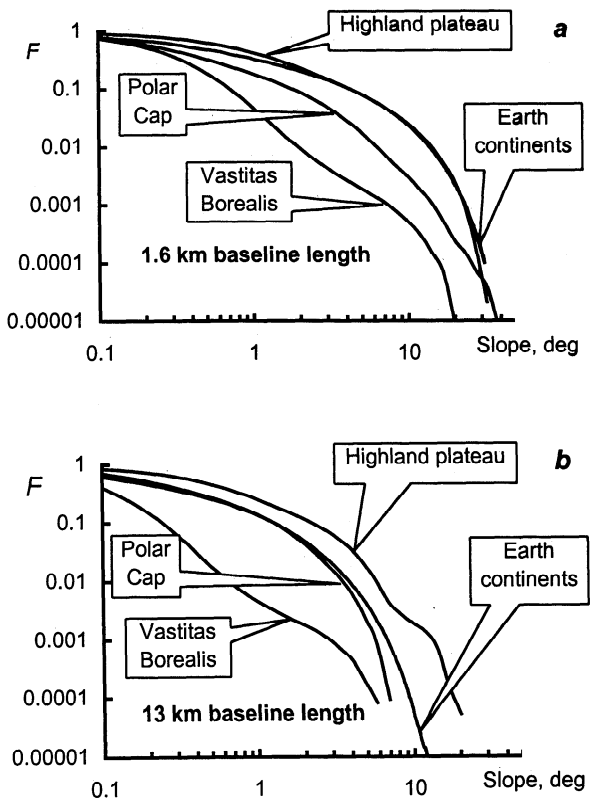


**Figure 11.** Steep-slope tails of the cumulative slope-frequency distributions. Logarithmic scale on both axes. Baseline length used is (a) 1.6 km for Mars and 1.9 km for the Earth, and (b) 12.8 km for Mars and 14.8 km for the Earth.

The Highland Plateau is represented by a set of units marked as $Npl_1$, $Npl_2$, Npld, Nple, Nplh, Nplr in the geologic maps. The highland plateau has a relatively large number of steep slopes. The rough topography of this old terrain is known to be inherited from heavy bombardment. The presence of steep slopes here shows that this terrain can maintain steep slopes for a geologically long time.

For the polar cap curve in Figure 11 we took both ice (Api) and layered (Apl) polar deposits. The polar cap is generally smoother than the highlands. For short baselines (Figure 11a), it has a deficit of 1°-10° slopes in comparison to the highland plateau. The polar cap is thought to be made of ice-dominated material [e.g., *Thomas et al*, 1992]. Ice is much more ductile than silicate rocks. The ice-rich material of the polar cap probably cannot retain steep slopes, and relaxation processes may occur [e.g., *Zuber et al.*, 1998]. However, extremely steep slopes (>20°) in the polar cap are as frequent as in the highlands. These slopes are related to the major polar cap marginal scarp, troughs, and Chasma Boreale. The presence of such steep slopes in the presumably ductile material of the polar cap may provide evidence for some recent or ongoing slope-forming processes [e.g., *Zuber et al.*, 1998]. For longer baselines (Figure 11b) the polar cap does not have extremely steep slopes. This is partly because the total height difference here is only 1-2 km, a few times smaller than that for highlands.

Figure 11 also shows the distribution of the steep slopes on Earth continents derived from the GTOPO30 digital elevation model described above. For short baselines, steep slopes on Earth are as frequent as those on martian highlands. With increasing baseline length, the proportion of steep slopes on Earth decreases much faster than that for martian highlands (compare Figures 11a and 11b). The difference is partly due to the somewhat smaller general topography amplitude on Earth than on Mars. The presence of abundant large impact craters on Mars is another obvious reason for this difference. Erosion by water on Earth, effectively producing short steep slopes, also contributes to the difference.

### 6.2. The Steepest Slopes

For kilometer-scale baselines, slopes steeper than the angle of repose are scarce. Such slopes indicate either relative youth or an unusual mechanical strength of the material. Studying the steepest slopes with MOLA data, one needs to take into account that the slopes are measured along profile. The measured slope of a linear scarp will be steeper if the scarp is normal to the MOLA pass and gentler if the pass crosses the scarp at some angle. This means that MOLA data, with their present between-profile density, do not permit an exhaustive search to be made for the steepest slopes, even in the areas of presently relatively dense spacing of profiles.

We searched the complete MOLA data set for the steepest point-to-point slopes. We found that a total of 105 point-to-point segments have slopes steeper than 35°. Nine of these are probably data errors associated with some processing problems or caused by near-surface haze or clouds. The rest are associated with apparently steep features on the surface. The numbers of the steep segments associated with features of different types are listed in Table 1, and some examples are shown in Figure 12. We grouped the features in the following classes: impact craters, the polar cap scarps (Figure 12c), Olympus Mons and its aureole, tectonic (Figures 12a and 12b) and erosion features. The slopes of steep segments are sorted according to these feature classes in Figure 3.

**Table 1.** The Steepest Slopes on Mars

| Feature Type | Number of Segments Steeper Than 35° | Number of Segments Steeper Than 40° |
|---|---|---|
| Impact craters | 6 | 0 |
| The polar cap scarp | 38 | 19 |
| Chasma Boreale | 18 | 11 |
| The scarp itself | 20 | 8 |
| Olympus Mons scarp and aureole | 10 | 1 |
| Olympus Mons scarp | 1 | 0 |
| $Aoa_4$ | 8 | 1 |
| $Aoa_3$ | 1 | 0 |
| Grabens, channels, fretted terrains | 42 | 10 |
| Elysium Fossae | 9 | 1 |
| Grabens around Alba Patera | 4 | 1 |
| Acheron Fossae | 1 | 0 |
| Valles Mariners | 7 | 2 |
| Noctis Labyrintus | 11 | 2 |
| Kasei Valles | 4 | 0 |
| Fretted terrains | 6 | 4 |
| Suspected erroneous data | 9 | 8 |

$Aoa_4$, $Aoa_3$, the uppermost geological units in Olympus Mons aureole according to *Scott and Tanaka* [1986].

**6.2.1. Impact craters.** Only six steep measured segments of impact crater walls have slopes steeper than 35°, and none of them are steeper than 38°. Crater walls are formed during the modification stage of crater formation [e.g., *Melosh*, 1989], when surface material is mobilized after the shock wave has passed. In this situation, walls with slopes steeper than the angle of repose cannot easily be formed. This agrees with the observed absence of extremely steep slopes for the crater walls.

**6.2.2. Tectonic and erosion features.** The steepest segments in tectonic and erosion features are usually parts of very high scarps (more than 1 km high). For these scarps, as well as for the crater walls, the steepest segments of slopes tend to be in the upper part of the scarp (Figures 12a and 12b). This can be relatively easily understood in terms of slope processes: mass-wasted material forms relatively gentler slope near the scarp base, while active downward sliding of material favors steeper intermediate to upper parts of the scarps, and bedrock cliffs, from which debris is being weathered and shed, have the highest slopes. Although the orbits cross virtually all graben systems in the northern hemisphere, only a few graben systems display very steep slopes in MOLA profiles. The orbits cross several outflow channels in the northern hemisphere, but only Kasei Valles has very steep slopes.

**6.2.3. Olympus Mons aureole.** In the Olympus Mons aureole the steepest slopes are observed predominantly in the youngest subdivision of *Scott and Tanaka* [1986], unit $Aoa_4$, although orbits also cross other subdivisions. This difference seems most plausibly attributed to slope degradation with time.

**6.2.4. The polar cap.** A large number of the steepest slopes in the polar cap (Table 1, Figure 3) may be explained partly by the high concentration of MOLA measurements at the region of multiple orbit crossings at high latitudes. In any case, it is seen that the polar cap scarp does have very steep slopes (Figure 12c) [*Zuber et al.*, 1998]. The upper part of Chasma Boreale is characterized by the steepest site in the po-

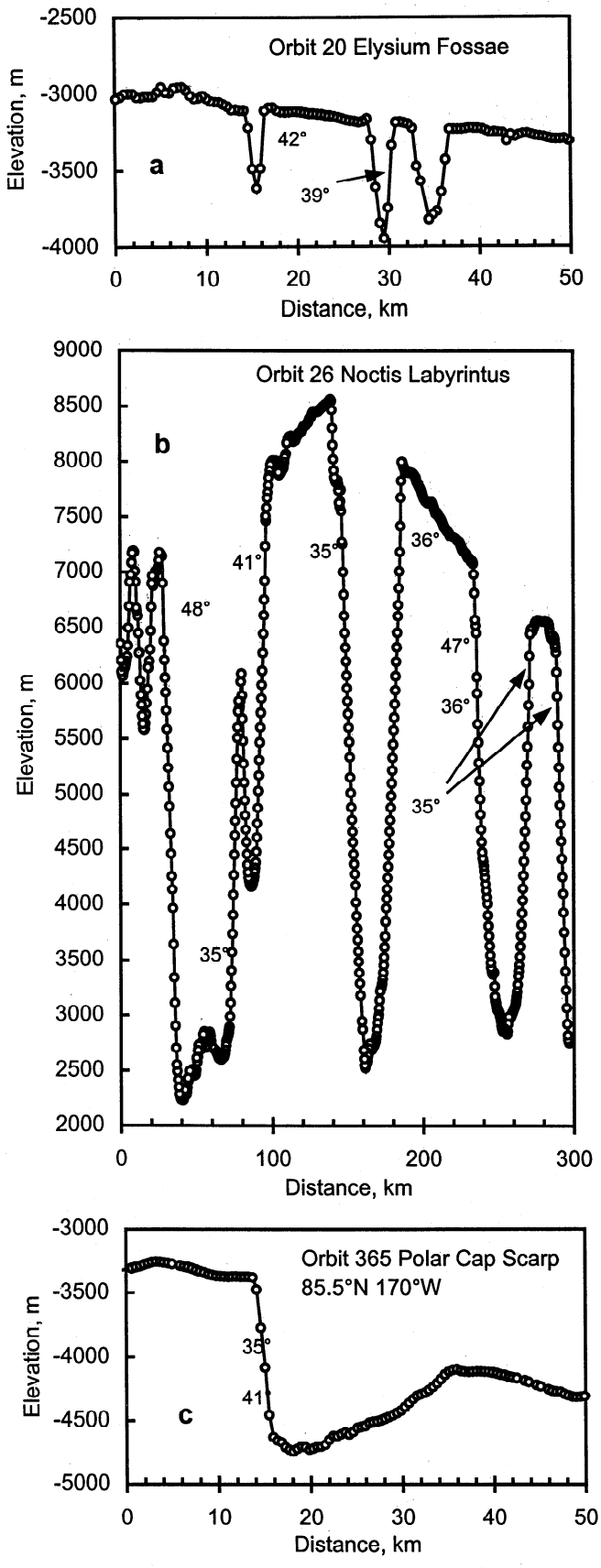


**Figure 12.** Sample profiles illustrating the location of some of the steepest slopes on Mars detected by MOLA: (a) section of orbit 20 in Elysium Fossae, (b) section of orbit 26 in Noctis Labyrithus, and (c) section of orbit 365 in the north polar cap region.

lar cap and in the entire surveyed part of the surface. Once again, the presence of the extremely steep slopes in this material is evidence for young and/or dynamically formed steep topography.

## 7. Conclusions

1. Martian surface slopes can be calculated at baselines from 0.4 to 25 km using MOLA profiles and compared to assess general behavior and relation to geologic units.

2. Median slope is proposed as a characteristic measurement of the typical surface roughness at each corresponding scale and is favored over RMS slope because it is not influenced by the small number of higher slopes at the upper end of the slope-frequency distribution tail.

3. Median slope complements interquartile roughness characterization in that it is more sensitive to smaller baseline slopes.

4. Maps of the median slopes of the northern hemisphere of Mars can be used to characterize typical kilometer-scale roughness for a set of geologic units mapped in the northern hemisphere. This analysis demonstrates that many individual units and groups of units are characterized by distinctive surface slopes, and that these characteristics are sufficiently different that they hold promise for use in the definition and characterization of units.

5. Characterization of the slope properties of geological units provides information useful in the interpretation of their origin and evolution. The generally smooth topography of the diverse Vastitas Borealis Formation is dominated by about 3 km, 0.3° steep features, and this unit differs distinctly from other geological units on Mars. The similarity of roughness characteristics of the several highland plateau units suggests that kilometer-scale topography was largely inherited from the period of heavy bombardment. The northern polar cap and layered terrains are largely very smooth at small scale.

6. The long, steep-sloped tails of the slope-frequency distributions are compared for the dominant terrain types on Mars and Earth continents. Terrestrial continents are smoother than cratered highlands but rougher than the Vastitas Borealis Formation and most volcanic plains. No global or regional topography data for terrestrial planets have a resolution and accuracy sufficient for comparison of slope statistics with MOLA data, except the topography of vast land areas on the Earth, and some seafloor data.

7. All observed slopes much steeper than the angle of repose are located; steep slopes occur in the upper parts of tectonic scarps, most likely representing bedrock exposures, in a few crater interiors, and in the presumably ductile polar cap (suggesting geologically recent and/or ongoing formation of these polar cap slopes).

**Acknowledgments.** We gratefully acknowledge the fundamental work of the MOLA engineering team and the Mars Global Surveyor Project in making this experiment a success. This work was performed with financial support from the Mars Global Surveyor Project through the MOLA team, a grant from the Mars Data Analysis Program (NAG 5-8283), and a grant from the Mars Landing Site Selection Program (NAG 5-4231). We gratefully acknowledge fruitful discussions with Oded Aharonson and very helpful reviews from Gregory A. Neumann and an anonymous reviewer. Thanks are extended to Anne Côté, who helped in manuscript production.

## References

Aharonson, O., M. T. Zuber, G. A. Neumann, and J. W. Head, Mars: Northern hemisphere slopes and slope distributions, *Geophys. Res. Lett., 25*, 4413-4416, 1998.

Aharonson, O., M. T. Zuber, and G. A. Neumann, Second order statistics of topography of the northern hemisphere of Mars from MOLA, *Lunar Planet. Sci.* [CD-ROM], *XXX*, abstract 1792, 1999.

Albee, A. L., F. D. Palluconi, and R. E. Arvidson, Mars Global Surveyor Mission: Overview and status, *Science, 279*, 1671-1672, 1998.

Clark, P. E., M. A. Leake, and R. F. Jurgens, Goldstone radar observations of Mercury, in *Mercury*, edited by F. Vilas, C. R. Chapman and M. S. Matthews, pp. 77-100, Univ. of Ariz. Press, Tucson, 1988.

Cooper, C. D., and J. F. Mustard, Topography and roughness signatures of erosion of crusted soils on Mars, *Lunar Planet. Sci.* [CD-ROM], *XXX*, abstract 1999, 1999.

Defense Mapping Agency, *Defense Mapping Agency Product Specifications for Digital Terrain Elevation Data (DTED)*, 26 pp., Defense Mapping Agency Aerospace Cent., St. Louis, Mo., 1986.

Dial, A. L., Geologic map of the Mare Boreum region of Mars, *U.S. Geol. Surv. Misc. Inv. Map, I-1640*, 1984.

Fishbaugh, K. E., and J. W. Head, North polar region of Mars: Topography of circumpolar deposits and sediments based on Mars Orbiter Laser Altimeter (MOLA) data, *Lunar Planet. Sci.* [CD-ROM], *XXX*, abstract 1401, 1999.

Ford, P. G., and G. H. Pettengill, Venus topography and kilometer-scale slopes, *J. Geophys. Res., 97*, 13,103-13,114, 1992.

Frey, F., S. E. Sakimoto, and J. Roark, The MOLA topographic signature at the crustal dichotomy boundary zone on Mars, *Geophys. Res. Lett., 25*, 4409-4412, 1998.

Garvin, J. B., and J. J. Frawley, Geometric properties of Martian impact craters: Preliminary results from the Mars Orbiter Laser Altimeter, *Geophys. Res. Lett., 25*, 4405-4408, 1998.

Garvin, J. B., J. J. Frawley, and J. B. Abshire, Vertical roughness of Mars from the Mars Orbiter Laser Altimeter, *Geophys. Res. Lett., 26*, 381-384, 1999.

Greeley, R., and J. E. Guest, Geological map of the eastern equatorial region of Mars, *U.S. Geol. Surv. Misc. Inv. Ser. Map, I-1802-B*, 1987.

Harmon, J. K., and D. B. Campbell, Radar observations of Mercury, in *Mercury*, edited by F. Vilas, C. R. Chapman, and M. S. Matthews, pp. 101-117, Univ. of Ariz. Press, Tucson, 1988.

Head, J. W., N. Seibert, S. Pratt, D. E. Smith, M. T. Zuber, S. C. Solomon, P. J. McGovern, J. B. Garvin, and the MOLA Science Team, Characterization of major volcanic edifices on Mars using Mars Orbiter Laser Altimeter data, *Lunar Planet. Sci.* [CD-ROM], *XXIX*, abstract 1322, 1998a.

Head, J. W., M. Kreslavsky, H. Hiesinger, M. Ivanov, S. Pratt, N. Seibert, D. E. Smith, and M. T. Zuber, Oceans in the past history of Mars: Tests for their presence using Mars Orbiter Laser Altimeter (MOLA) data, *Geophys. Res. Lett., 25*, 4401-4404, 1998b.

Kreslavsky, M. A., and J. W. Head, Frequency distribution of kilometer-scale slopes on Mars: Initial results from MOLA data, *Lunar Planet. Sci.* [CD-ROM], *XXX*, abstract 1190, 1999a.

Kreslavsky, M. A., and J. W. Head, Kilometer-scale roughness of geological units on Mars: Initial results from MOLA data, *Lunar Planet. Sci.* [CD-ROM], *XXX*, abstract 1191, 1999b.

Masursky, H., and N. L. Crabill, Search for the Viking 2 landing site, *Science, 194*, 62-68, 1976.

McEwen, A., M. Malin, L. Keszthelyi, P. Lanagan, R. Beyer, and W. Hartmann, Recent and ancient flood lavas on Mars, *Lunar Planet. Sci.* [CD-ROM], *XXX*, abstract 1829, 1999.

Melosh, H. J., *Impact Cratering: A Geologic Process*, Oxford Univ. Press, New York, 1989.

Parker, T. J., R. S. Saunders, and D. M. Schneeberger, Transitional morphology in West Deuteronilus Mensae, Mars: Implication for modification of the lowland-highland boundary, *Icarus, 82*, 111-145, 1989.

Parker, T. J., D. S. Gorsline, R. S. Saunders, D. Pieri, and D. M. Schneeberger, Coastal geomorphology of the Martian northern plains, *J. Geophys. Res., 98*, 11,061-11,078, 1993.

Scott, D. H., and K. L. Tanaka, Geological map of the western equatorial region of Mars, *U.S. Geol. Surv. Misc. Inv. Ser. Map, I-1802-A*, 1986.

Simpson, R. A., J. K. Harmon, S. H. Zisk, T. W. Thompson, and D. O. Muhleman, Radar determination of Mars surface properties, in *Mars*, edited by H. H. Kieffer, B. M. Jakosky, C. W. Snyder, and M. S. Matthews, pp. 686-729, Univ. of Ariz. Press, Tucson, 1992.

Smith, D. E., M. T. Zuber, G. A. Neumann, and F. G. Lemoine, Topography of the Moon from the Clementine lidar, *J. Geophys. Res.*, 102, 1591-1611, 1997.

Smith, D. E., et al., Topography of the northern hemisphere of Mars from the Mars Orbiter Laser Altimeter (MOLA), *Science, 279*, 1686-1692, 1998.

Tanaka, K. L., and D. H. Scott, Geological map of the polar regions of Mars, *U.S. Geol. Surv. Misc. Inv. Ser. Map, I-1802-C*, 1987.

Thomas, P., S. Squyres, K. Herkenhoff, A. Howard, and B. Murray, Polar deposits of Mars, in *Mars*, edited by H. H. Kieffer, B. M. Jakosky, C. W. Snyder, and M. S. Matthews, pp. 767-795, Univ. of Ariz. Press, Tucson, 1992.

Tyler, G. L., R. A. Simpson, M. J. Maurer, and E. Holmann, Scattering properties of the Venusian surface: Preliminary results from Magellan, *J. Geophys. Res., 97*, 13,115-13,139, 1992.

U.S. Geological Survey, *Digital Elevation Models: Data User Guide 5*, 50 pp., Reston, Va., 1993.

Van der Vaerden, B. L., Mathematical Statistics, Springer-Verlag, New York, 1969.

Zuber, M. T., D. E. Smith, J. W. Head, D. O. Muhleman, S. C. Solomon, J. B. Garvin, J. B. Abshire, and J. L. Bufton, The Mars Observer laser altimeter investigation, *J. Geophys. Res., 97*, 7781-7797, 1992.

Zuber, M. T., et al., Observation of the north polar region of Mars from the Mars Orbiter Laser Altimeter, *Science, 282*, 2053-2060, 1998.

---

J. W. Head and M. A. Kreslavsky, Department of Geological Sciences, Brown University, Box 1846, Providence, RI 02912.

(Received March 30, 1999; revised June 16, 1999;
accepted June 22, 1999.)